



HAL
open science

Effects of water and fines contents on the resilient modulus of the interlayer soil of railway substructure

Trong Vinh Duong, Yu-Jun Cui, Anh Minh A.M. Tang, Jean Claude Dupla,
Jean Canou, Nicolas Calon, Alain Robinet

► **To cite this version:**

Trong Vinh Duong, Yu-Jun Cui, Anh Minh A.M. Tang, Jean Claude Dupla, Jean Canou, et al.. Effects of water and fines contents on the resilient modulus of the interlayer soil of railway substructure. *Acta Geotechnica*, 2016, 11 (1), pp.51-59. 10.1007/s11440-014-0341-0 . hal-01271097

HAL Id: hal-01271097

<https://enpc.hal.science/hal-01271097>

Submitted on 25 Apr 2018

HAL is a multi-disciplinary open access archive for the deposit and dissemination of scientific research documents, whether they are published or not. The documents may come from teaching and research institutions in France or abroad, or from public or private research centers.

L'archive ouverte pluridisciplinaire **HAL**, est destinée au dépôt et à la diffusion de documents scientifiques de niveau recherche, publiés ou non, émanant des établissements d'enseignement et de recherche français ou étrangers, des laboratoires publics ou privés.

35 **Abstract**

36 This paper deals with the resilient behavior of the interlayer soil which is created mainly by the
37 interpenetration of ballast and sub-grade soils. The interlayer soil studied was taken from a site in
38 the South-East of France. Large-scale cyclic triaxial tests were carried out at three water contents
39 ($w = 4, 6$ and 12%) and three fines contents corresponding to 5% sub-grade added to the natural
40 interlayer soil, 10% sub-grade added to the natural interlayer soil and 10% fine particles (< 80
41 μm) removed from the natural interlayer soil. Soil specimens underwent various deviator stresses,
42 and for each deviator stress a large number of cycles were applied. The effects of deviator stress,
43 number of cycles, water content and fines content on the resilient modulus (M_r) were analyzed. It
44 appears that the effects of water content and fines content must be analyzed in a global fashion
45 because the two effects are closely linked. Under unsaturated conditions, the soil containing high
46 fines content has higher resilient modulus due to the contribution of suction. When the soil
47 approaches the saturated state, it loses its mechanical performance with a sharp decrease in
48 resilient modulus.

49 *Keywords:* railway sub-structure; interlayer soil; resilient modulus; fines content; water content;
50 large-scale cyclic triaxial test.

51

52 **Introduction**

53 The soils in the sub-structures of highway and railway are subjected to a huge number of traffic
54 loading cycles. In this context, the resilient modulus of sub-structure soils is an important
55 parameter to be considered when designing new tracks or when maintaining under-operation
56 tracks. Indeed, several authors [1, 4, and 28] reported that the resilient modulus of sub-grade can
57 strongly influence the mechanical behavior of sub-structure.

58 For the French ancient railway tracks constructed in the 1880s, as ballast was placed
59 directly on the sub-grade during the construction without any separation layers, an interlayer was
60 naturally created over time mainly by the interpenetration of ballast and sub-soil under the traffic
61 effect [5-7, 32]. This interlayer has been kept as part of the sub-structure considering its high
62 mechanical performance related to its high unit mass [33]. As the interlayer is a “component” of
63 the sub-structure overlying the sub-grade, its mechanical behavior appears to be of primary
64 importance for the overall behavior of sub-structure even the overall track structure. However,
65 because this material has been formed naturally, it can present large variability in terms of fines
66 natures and fines contents. Moreover, under the effect of climatic conditions, soil water content
67 changes also constantly. These changes in fines content, fines nature and water content can
68 greatly affect soil mechanical behavior such as soil resilient modulus.

69 The notion of resilient behavior appeared for the first time in the middle of the 20th
70 century [16, 17]. In the railway context, the resilient modulus (M_r) is defined as the secant slope
71 of the curve of deviator stress versus axial strain obtained from cyclic triaxial tests [21, 26-28, 30,
72 and 37]. Previous studies showed that there are several factors that affect the resilient modulus of
73 unbound granular materials, in particular the stress level [14, 22, 24, 26, and 30]. The increase in
74 moisture content appears to decrease the resilient modulus [10, 11, and 14]. For the effect of

75 loading cycles, a large disagreement exists in terms of number of cycles required to reach the
76 stabilization of resilient modulus [23, 24, 30, 35, 36]. As far as the effect of fines content is
77 concerned, there is no conclusive observation as mentioned by Lekarp et al. [24]. Thom and
78 Brown [31] and Kamal et al. [20] reported that the resilient modulus generally decreases when
79 the fines content increases. However, Jorenby and Hicks [19] observed that the stiffness of
80 crushed aggregate has an initially increase trend followed by a considerable reduction when
81 clayey fines content increased.

82 All these factors (moisture content, fines content, number of cycles) influence the resilient
83 response of materials. However, to the authors' knowledge, their combined effect has rarely
84 investigated especially for the interlayer soil. In the present work, large-scale cyclic triaxial tests
85 were carried out to study the variations of M_r of an interlayer soil under the combined effects of
86 stress level, water content, fines content and cyclic loadings.

87 **Materials and methods**

88 The studied interlayer soil was taken from S nissiat, near Lyon, France. The grain size
89 distribution curves of the natural interlayer soil (ITL_0) and the sub-grade soil (SG) are presented
90 in Fig. 1. It can be observed that the interlayer soil has a large fines content (16% of particles are
91 smaller than 80 μm), and its grain size distribution curve is well graded from ballast size (60 mm)
92 to clay size ($< 2 \mu\text{m}$). Its physical properties (density, plasticity index, blue methylene value and
93 proctor curve) of this material were reported by Trinh et al. [33, 34]. For the SG, almost all soil
94 particles are smaller than 80 μm .

95 In order to study the influence of fines content, the fines content of the soil was varied by
96 either removing fine particles smaller than 80 μm from the interlayer soil (-10% for ITL_{-10}) or
97 adding sub-grade soil into the interlayer soil (+5% for ITL_5 and +10% for ITL_{10}). The percentages

98 refer to the ratio of dry mass of fine particles to dry mass of interlayer soil. The removal of fine
99 particles for the preparation of *ITL₁₀* was done by sieving. The grain size distribution curves of
100 *ITL₁₀*, *ITL₅* and *ITL₁₀* are also shown in Fig. 1.

101 For the specimen preparation, water were first added and mixed with the material using a
102 large mixer to reach the target water content. After mixing, the wet materials were stored in
103 hermetic containers for at least 24 h for moisture homogenization. Compaction was performed in
104 6 layers of 0.1 m thick each using a vibratory hammer to a dry unit mass of 2.01 Mg/m³. This is
105 the maximum dry unit mass which can be reached in the adopted conditions without breaking
106 ballast particles.

107 Because large particles were involved, a large-scale triaxial apparatus developed by Dupla
108 et al. [8] was used, enabling specimens of 300 mm in diameter and 600 mm in height to be tested.
109 This apparatus can apply large number of loading cycles (up to several millions) at a frequency
110 up to several tens of Hertz.

111 The program of tests is presented in Table 1. All the four soils were tested at three water
112 contents ($w = 4\%$; 6% and 12%) corresponding to three initial degrees of saturation ($S_{ri} = 32\%$;
113 49% and 100%), except *ITL₅* on which only one test at a water content of $w = 6\%$ was conducted
114 owing to lack of material. The tests are named according to the material (*ITL₁₀*, *ITL₀*, *ITL₅*, *ITL₁₀*)
115 and water content. For instance, *ITL₀w4* corresponds to the test on *ITL₀* at 4% water content. To
116 overcome the problem related to the limited material quantity, the multi-step loading procedure
117 proposed by Gidel et al. [12] was adopted. This procedure enables several deviator stress levels to
118 be applied before the soil specimen reaches the failure state, thereby reducing the number of tests
119 on one hand and avoiding the effect of variability of soil specimens on the other hand.

120 The cyclic triaxial tests were performed under a constant confining pressure $\sigma_3 = 30$ kPa.
121 This value was chosen by referring to the wheel load generated by train [2], the depth of the
122 interlayer (from 250 mm to 600 mm), the Poisson's ratio (0.3 - 0.4 as proposed by Selig and
123 Waters [28]). The vertical stress at the top of interlayer was found to be 40 to 90 kPa. These
124 values correspond to the Indian railways as reported by Jain and Keshav [18] and American
125 railways as reported by Selig and Waters [28] and Yang et al. [39]. In other countries where
126 heavier wagons are used, the wheel load may reach 30 tons per axle [2], leading to a vertical
127 stress of 120 to 140 kPa on the interlayer [13, 18, 25]. In this study, a maximum deviator stress of
128 200 kPa was applied. All the tests were performed under drained condition; the valves were open
129 (under unsaturated condition) or connected to a water back pressure source (under saturated
130 condition). During the saturated triaxial test, the back pressure was kept constant and pore water
131 can drain freely. For the loading frequency, a value of 5 Hz was chosen because this is the
132 dominant one among a number of frequencies generated in the French ancient sub-structures at a
133 train speed of 100 km/h [29]. During the tests, the deviator stress was increased in steps from 0 to
134 various target values; in each step, 30 000 cycles were applied and the variations of axial strain
135 were recorded.

136 **Results**

137 Fig. 2 presents typical curves of deviator stress versus axial strain for the first cycles in test
138 *ITL_{5w6}*. It also shows the definition of permanent axial strain (ϵ_p), the resilient axial strain (ϵ_r)
139 through the first cycle. It can be observed that the minimum deviator stress did not totally reach
140 zero for all cycles. This was probably due to the high loading/unloading speed (frequency of 5
141 Hz) that caused a delay between the target signal and the real signal. However, it is believed that

142 this problem does not affect the resilient modulus (M_r) that corresponds to the secant slope of
143 curves (see Fig. 2).

144 Fig. 3 plots the deviator stress versus the axial strain for the moments where the values of Δq_{max}
145 were increased: during the first 8 cycles ($N = 8$) under $\Delta q_{max} = 45$ kPa (Fig. 3a), from $\Delta q_{max} = 45$
146 kPa ($N = 30\,000$) to $\Delta q_{max} = 90$ kPa ($N = 30\,001 - 30\,0004$) (Fig. 3b), from $\Delta q_{max} = 90$ kPa ($N =$
147 $60\,000$) to $\Delta q_{max} = 145$ kPa ($N = 60\,001 - 60\,0004$) (Fig. 3c) and from $\Delta q_{max} = 145$ kPa ($N =$
148 $90\,000$) to $\Delta q_{max} = 20$ kPa ($N = 90\,001 - 90\,0004$) (Fig. 3d). It can be observed that when a new
149 deviator stress was applied, the axial strain increased accordingly. During the very first cycles
150 under each stress level, the loading and unloading paths did not form close cycles, suggesting that
151 significant permanent axial strain developed. In this case, the resilient modulus was determined
152 based on the unloading path of a cycle and the loading path of the next cycle. The hysteresis loop
153 was large in the first cycles, and with the increase of number of cycles, this hysteresis became
154 less and less significant. At large number of cycles by the end of each loading level, the material
155 behaved almost in a purely elastic fashion. Werkmeister et al. [38] reported that the change in the
156 loop shape provides information about the different deformation mechanisms. In the beginning,
157 there was probably particles rotation and rearrangement producing the plastic strain. Over time,
158 these particles movements became limited and a purely resilient state is reached where strain is
159 due to the deformation at the contacts of particles. Note that the shape of loading/unloading loops
160 is related to the slope adopted for the determination of the resilient modulus. When two paths
161 formed a close cycle, the straight line between the lowest and highest point of the
162 loading/unloading cycle was used in the determination.

163 Fig. 4 depicts the evolution of resilient strain with number of cycles for test *ITL_{2w12}*.
164 When the deviator stress increased, the resilient strain increased sharply during the first cycles of

165 each stress level, and decreased afterwards to reach stabilization. The resilient strain was larger
166 under higher deviator stress.

167 Fig. 5 depicts the variations of M_r with the number of cycles (N) at three water contents
168 and various deviators stress levels for ITL_{10} . In the case of ITL_{10w4} (Fig. 5a) at $\Delta q_{max} = 23$ kPa,
169 the data of resilient modulus shows some scatter, but in general an increase trend can be
170 identified. Because of the data scatter, it is difficult to determine the number of cycles at which
171 the stabilization of resilient modulus started. The values in other stress levels are more or less
172 constant around 250 MPa. For ITL_{10w6} (Fig. 5b), the resilient modulus for all stress levels are
173 found to increase significantly in the beginning and then stabilize after around 15 000 cycles.
174 When Δq_{max} was increased from 45 kPa to 90 kPa, the resilient modulus rose up sharply. By
175 contrast, an opposite trend was observed when Δq_{max} was increased from 90 to 140 kPa. It can be
176 seen from Fig. 5c that for each deviator stress level, the resilient modulus decreased during the
177 first cycles. For instance, it decreased from 168 MPa to 144 MPa from cycle 1 to cycle 7.
178 However, this decreasing trend came very quickly to its end and was replaced by an increasing
179 one. Afterwards, the increase rate slowed down and the resilient modulus value tended to
180 stabilize after about 5000 loading cycles. Referring to Fig. 4, the significant variations of resilient
181 modulus in Fig. 5 correspond to the phase characterized by quick development of resilient axial
182 strain just after the change of stress level, and the stabilization states of resilient modulus
183 corresponds to the stabilization of resilient axial strain.

184 These observations are confirmed in the case of ITL_{5w6} (see Fig. 6). For all stress levels, the
185 resilient modulus increased with the number of cycles during the first cycles. At $\Delta q_{max} = 45$ kPa
186 about 10 000 cycles were needed for the resilient modulus to become stable while at $\Delta q_{max} = 140$
187 kPa and 200 kPa, about 5000 cycles were needed. The variation range of M_r at all stress levels is

188 about ± 10 MPa. On the whole, the effect of deviator stress is not as clear as in the case of
189 *ITL₁₀w6*.

190 The results of *ITL₀* are presented in Fig. 7. The variation of M_r with N is more pronounced in the
191 case of *ITL₀w12* (Fig. 7c) than in the cases of *ITL₀w4* (Fig. 7a) and *ITL₀w6* (Fig. 7b). After the
192 first variations when the deviator stress Δq_{max} changed, the resilient modulus increased with the
193 number of cycles in the case of *ITL₀w12*, while the changes in the two other cases are not clear.

194 As regards *ITL₋₁₀*, the results with three different water contents are presented in Fig. 8. In the
195 two cases of $w = 4\%$ and 12% , the resilient modulus did not vary much for the deviator stress up
196 to 90 kPa, suggesting an insignificant influence of the number of cycles. Also, the influence of
197 Δq_{max} is insignificant because albeit the variation of Δq_{max} , the resilient modulus remained at a
198 steady value: about 230 MPa for *ITL₋₁₀w12* and 250 MPa for *ITL₋₁₀w4*. In the case of $w = 6\%$
199 (Fig. 8b), the variation is clearer as the results show a slight increasing trend of M_r with the
200 number of cycles and Δq_{max} . At the stress level of 140 kPa, there was a sharp decrease of M_r ,
201 regardless of the water content: for the three tests, when Δq_{max} was increased from 90 kPa to 140
202 kPa, a reduction of M_r of about 50 kPa was produced. Afterwards, the variations of resilient
203 modulus with the number of cycles became much more pronounced than in the cases of other
204 deviator stress levels.

205 **Discussions**

206 From the test results, it was observed that after a few scattered results at the beginning of each
207 stress level, the resilient modulus became stable with the number of cycles. However, the
208 variations were different for different soils and different water contents. The variations were clear
209 in the case of *ITL₁₀* (Fig. 5b and c), insignificant in the first part of test *ITL₀w4* (Fig. 7a) and *ITL*.

210 $_{10}w4$ (Fig. 8a). The stabilization value was reached right after the first cycles in test $ITL_{0}w4$ (see
211 Fig. 7a) and after 15 000 cycles in test $ITL_{10}w6$ (see Fig. 5b). Therefore, it can be stated that the
212 number of cycles needed for M_r to reach stabilization depends on the stress level, water content,
213 and fines content. This can explain the disagreement found in literature regarding the number of
214 cycles required to attain a stable resilient state: Stewart [30] studied the ballast behavior and
215 reported a stabilization after 1000 cycles while Hicks and Monismith [14] and Allen and
216 Thompson [3] (cited by Lekarp et al. [24] and Lackenby [23]) observed that 50 – 100 cycles are
217 needed for the stabilization for granular materials.

218 The variations of resilient modulus during the scattered phase at the beginning of each Δq_{max} were
219 observed in all tests. This phase corresponds to the stage where the permanent axial strain
220 developed quickly and the loading/unloading path did not form a close cycle in the deviator stress
221 – axial strain plane. This can be explained as follows: when Δq_{max} was increased, the soil
222 behavior became elasto-plastic; thus irreversible strain was produced. However, this phenomenon
223 occurred during the first loading. Afterwards, the cyclic loading led to a progressive stabilization
224 of the particles arrangement, thereby a negligible plastic strain.

225 For a better analysis on the effects of deviator stress and water content, the end-level resilient
226 modulus values (after 30 000 cycles for each deviator stress level) are plotted versus deviator
227 stress in Fig. 9. For ITL_{10} (Fig. 9a), the results at 4% and 12 % water contents present a slight
228 decrease of resilient modulus when the deviator stress was increased from 23 to 102 kPa. On the
229 contrary, in the case of 6% water content, the resilient modulus increased and then reached
230 stabilization. The values of 4% and 6% water contents fall in the same range, around 250 MPa
231 and clearly higher than the values of 12% water content. For ITL_0 (Fig. 9b), at 4% and 6% water
232 content, the resilient modulus increased with the deviator stress and the values of 4% are higher

233 than those of 6%. The values of ITL_0 in near saturated state ($w = 12\%$) are, as opposed to the case
234 of ITL_{10} , higher than those of 4% water content. In the case of ITL_{-10} (Fig. 9c), the curves have
235 almost the same shape: a stage of slight variations up to 90 kPa of deviator stress followed by a
236 stage of decrease, the decrease being more pronounced in the case of ITL_{-10w12} .

237 In terms of water content effect, the value of ITL_{-10} at 4% water content is the highest; the values
238 of 12% water content are lower than those of 4% water content but higher than those of 6% water
239 content. The relative positions of these curves show that the water content effect is not the same
240 for the three materials. It appears that the increase of water content brings a negative effect to the
241 resilient modulus of the soil that has the highest fines content (ITL_{10}). However, for ITL_0 and ITL_{-10} ,
242 the resilient modulus decreased when water content changed from 4% to 6% but increased
243 when water content was increased to 12%. Note that only a decreasing trend of resilient modulus
244 with growing saturation level for granular material was observed by Lekarp [24]. More studies
245 are required to clarify this issue.

246 For ITL_{-10} , a deviator stress of 90 kPa appears to be the critical value for the variations of
247 resilient modulus: all tests showed a decrease of resilient modulus at this stress level, suggesting
248 a significant change in soil behavior. As mentioned previously, after a certain number of cycles,
249 the resilient behavior was mainly governed by the contacts of soil particles. When the imposed
250 deviator stress increased, the stress applied at the inter-particles contact exceeds its limit and
251 particle breakage may occur. As a result, a sharp decrease of M_r is produced. This could be the
252 case for ITL_{-10} that has the lowest fines content. For ITL_0 and ITL_{10} , this phenomenon of particle
253 breakage was probably attenuated, leading to much smaller decrease of M_r .

254 As far as the effect of water content is concerned, the results show that the relative
255 positions of the curves of three different water contents are not the same for the three materials.
256 This suggests that the soil composition can strongly influence the material resilient modulus. Fig.
257 10 presents the results according to the water content: 4%; 6% and 12% in Figs. a, b and c,
258 respectively. The effect of fines content can be observed clearly. In the case of $w = 4\%$, the
259 results of ITL_{-10} and ITL_{10} are almost identical for the deviator stress up to 100 kPa. But much
260 lower values are observed for ITL_0 for the deviator stress up to 140 kPa. Beyond 140 kPa deviator
261 stress, the values become almost the same for ITL_{-10} and ITL_0 . At 6% water content, the resilient
262 modulus of ITL_0 is also the smallest, showing that when decreasing the fines content (from ITL_{10}
263 to ITL_0), a reduction of resilient modulus is produced. However, when the fines content is
264 decreased to a level as low as ITL_{-10} , the resilient modulus starts to increase. Under the near
265 saturation conditions ($w = 12\%$ in Fig. 10c), it is observed that the greater the fines content, the
266 lower the resilient modulus.

267 Fig. 11 plots the end stage resilient modulus at three stress levels with the variation of
268 water content and fines content. Despite of the scatter, it can be generally observed a clear trend
269 of M_r at all water content. It slightly decreases when the fine content added increases from -10% to
270 0%. After that, it can be observed a significant increase of M_r when the fine content added passes
271 to 10%. Adding more fine particles, in one hand, limited the contact between big particles contact
272 (ballast), but in other hand, increase the suction, as the gravimetric water content was kept
273 constant.

274 To identify the mechanisms of these phenomena, it appears necessary to consider the combined
275 effects of the fines content and the water content which is linked to the soil suction. It is well
276 known that for unsaturated soils, suction contributes to the soils shear strength, especially for the

277 fine-grained soils. This explains why fine particles show a positive effect on the resilient modulus
278 under unsaturated conditions, but a negative effect under saturated conditions. It can be observed
279 in the case of $\Delta q_{max} = 45$ kPa (Fig. 11a), for the case of 12% of water content, there was no more
280 suction effect, and the resilient modulus decrease with the increase of fine content. This implies
281 that in unsaturated conditions, due to the suction effect the interlayer soil containing high fines
282 content has a better mechanical performance, while in near saturation conditions, higher fines
283 contents leads to a significant degradation of mechanical performance. This is in agreement with
284 the observations of Huang et al. [15], Ebrahimi [9] and Duong et al. [7]. From a practical point of
285 view, these findings are important for the maintenance of railway tracks. If the soil containing
286 high fines content can satisfy the requirements in terms of resilient modulus under unsaturated
287 conditions, measures must be taken to protect it from water infiltration. Very often, it is a good
288 drainage system that should be set up for this purpose.

289 **Conclusions**

290 The resilient behavior of an interlayer soil taken in a railway sub-structure in France was studied
291 in the laboratory. The effects of deviator stress level, number of cycles, water content and fine
292 content were investigated by performing large-scale cyclic triaxial tests. Four fines contents and 3
293 water contents were considered.

294 At each deviator stress level, after the first scattered results due to the plastic behavior of
295 soil, the resilient modulus tended to stabilize with the number of cycles. It was found that the
296 number of cycles needed to reach stabilization depends on the material nature, water content and
297 stress level.

298 The effects of water content and of fines content are linked, and it appeared impossible to
299 distinguish the two effects. Indeed, in unsaturated conditions, due to the suction effect, the soil

300 having high fines content showed higher resilient modulus. On the contrary, when the soil
301 approached the saturated conditions, the fine particles provided a negative effect. This suggests
302 that drainage measures must be taken to protect the interlayer soil when its mechanical
303 performance appears satisfactory under unsaturated conditions but unsatisfactory under saturated
304 conditions.

305 **Acknowledgements**

306 This study was carried out within the research project RUFEX “Reuse and reinforcement
307 of ancient railway sub-structure and existing foundations”. The authors would like to address
308 their deep thanks to Ecole des Ponts ParisTech (ENPC), Railway Network of France (RFF),
309 French Railways Company (SNCF) and French National Research Agency for their supports.

310 **References**

- 311 1. ASSHTO (1993) Guide for design of pavement structures.
- 312 2. Alias J (1984) La voie ferrée. Techniques de construction et d'entretien. 2nd Ed.,
313 Eyrolles (In French).
- 314 3. Allen JJ, Thompson MR (1974) Resilient response of granular materials subjected to time
315 dependent lateral stresses. Transportation Research Record 510:1-13.
- 316 4. Basudhar PK, Ghosh P, Dey A, Valsa S, Nainegali LS (2010) Reinforced earth design of
317 embankment and cuts in railway. Research Designs and Standards Organization, Department of
318 Civil Engineering, Indian Institute of Technology Kanpur.
- 319 5. Cui YJ, Duong TV, Tang AM, Dupla J, Calon N, Robinet A (2013) Investigation of the
320 hydro-mechanical behaviour of fouled ballast. Journal of Zhejiang University- Science A,
321 14(4):244-255.
- 322 6. Duong TV, Trinh VN, Cui YJ, Tang AM, Calon N (2013a) Development of a large-scale
323 infiltration column for studying the hydraulic conductivity of unsaturated fouled ballast.
324 Geotechnical Testing Journal 36(1):1-10.
- 325 7. Duong TV, Tang AM, Cui YJ, Trinh VN, Dupla JC, Calon N, Canou J, Robinet A
326 (2013b) Effects of fines and water contents on the mechanical behavior of interlayer soil in
327 ancient railway sub-structure. Soils and Foundations (accepted for publications).

- 328 8. Dupla JC, Pedro LS, Canou J, Dormieux L (2007) Mechanical behaviour of coarse
329 grained soils reference. Bulletin de Liaison des Laboratoires des Ponts et Chaussées (268-
330 269):31-58.
- 331 9. Ebrahimi A (2011) Behavior of fouled ballast. Railway Track and Structures 107(8):25-
332 31.
- 333 10. Ekblad J, Isacsson U (2008) Influence of water and mica content on resilient properties of
334 coarse granular materials. International Journal of Pavement Engineering 9(3):215-227.
- 335 11. Ekblad J (2007) Influence of water on coarse granular road materials properties. PhD
336 dissertation, Royal Institute of Technology KTH, Stockholm, Sweden.
- 337 12. Gidel G, Hornych P, Chauvin JJ, Breysse D, Denis A (2011) A new approach for
338 investigating the permanent deformation behavior of unbound granular material using the
339 repeated load triaxial apparatus. Bulletin de Liaison des Laboratoires des Ponts et Chaussées
340 233:5-21.
- 341 13. Grabe P, Clayton C (2009) Effects of principal stress rotation on permanent deformation
342 in rail track foundations. Journal of Geotechnical and Geoenvironmental Engineering
343 135(4):555-565.
- 344 14. Hicks RG, Monismith CL (1971) Factors influencing the resilient response of granular
345 materials. Highway Research Record 345:15-31.

- 346 15. Huang H, Tutumluer E, Dombrow W (2009) Laboratory characterization of fouled
347 railroad ballast behavior. *Journal of the Transportation Research Board* 2117(1):93–101.
348 <http://dx.doi.org/10.3141/2117-12>.
- 349 16. Hveem FN (1955). Pavement deflections and fatigue failures. In *Highway research board*
350 *bulletin*, Highway Research Board 114:43–87.
- 351 17. Hveem FN, Carmany RM (1948) The factors underlying the rational design of pavements.
352 In *Highway Research Board Proceedings* 28:101–136.
- 353 18. Jain V, Keshav K (1999) Stress distribution in railway formation—a simulated study.
354 *Proceeding of the 2nd International Symposium on Pre-Failure Deformation Characteristics of*
355 *Geomaterials—IS Torino* pp. 653–658.
- 356 19. Jorenby BN, Hicks RG (1986) Base course contamination limits. *Transportation Research*
357 *Record* 1095, Transportation Research Board, Washington, D.C. pp.86–101.
- 358 20. Kamal MA, Dawson AR, Farouki OT, Hughes DAB, Sha’at AA (1993) Field and
359 laboratory evaluation of the mechanical behaviour of unbound granular materials in pavements.
360 *Transportation Research Record* 1406, Transportation Research Board, Washington, D.C. pp. 88–
361 97.
- 362 21. Kim D, Kim JR (2007) Resilient behavior of compacted subgrade soils under the repeated
363 triaxial test. *Construction and Building Materials* 21(7):1470–1479.
- 364 22. Kolisoja P (1997) *Resilient Deformation Characteristics of Granular Materials*. PhD
365 dissertation, Tampere University of Technology, Finland.

- 366 23. Lackenby J (2006) Triaxial behaviour of ballast and the role of confining pressure under
367 cyclic loading. PhD dissertation, University of Wollongong.
- 368 24. Lekarp F, Isacsson U, Dawson A (2000) State of the art. I: Resilient response of unbound
369 aggregates. *Journal of transportation engineering* 126(1):66–75.
- 370 25. Li D, Selig E (1998) Method for railroad track foundation design. I. Development.
371 *Journal of Geotechnical and Geoenvironmental Engineering* 124(4):316–322.
- 372 26. Lim WL (2004) Mechanics of railway ballast behaviour. PhD dissertation, University of
373 Nottingham.
- 374 27. Radampola S (2006) Evaluation and modelling performance of capping layer in rail track
375 substructure. Thesis dissertation, Central Queensland University.
- 376 28. Selig ET, Waters JM (1994) Track geotechnology and substructure management. Thomas
377 Telford.
- 378 29. SNCF (2009) R2520-2009-01 - Sollicitations mécaniques dans la plate-forme: Mesures
379 d'accélération verticales dans la plate-forme. Technical report (In French).
- 380 30. Stewart HE (1982) The prediction of track performance under dynamic traffic loading.
381 PhD Dissertation, University of Massachusetts.
- 382 31. Thom NH, Brown SF (1987) Effect of moisture on the structural performance of a
383 crushed-limestone road base. *Transportation Research Record* 1121, Transportation Research
384 Board, Washington, D.C. pp. 50–56.

- 385 32. Trinh VN (2011) Comportement hydromécanique des matériaux constitutifs de
386 plateformes ferroviaires anciennes. PhD Dissertation, Ecole Nationales des Ponts et Chaussées -
387 Université Paris – Est, France (In French).
- 388 33. Trinh VN, Tang AM, Cui YJ, Canou J, Dupla J, Calon N, Lambert L, Robinet A, Schoen
389 O (2011) Caractérisation des matériaux constitutifs de plate-forme ferroviaire ancienne. Revue
390 Française de Géotechnique (134-135): 65–74 (In French).
- 391 34. Trinh VN, Tang AM, Cui YJ, Canou J, Dupla J, Calon N, Lambert L, Robinet A, Schoen
392 O (2012) Mechanical characterisation of the fouled ballast in ancient railway track sub-structure
393 by large-scale triaxial tests. *Soils and Foundations* 52(3):511-523.
- 394 35. Uthus L, Hoff I, Horvli I (2005) A study on the influence of water and fines on the
395 deformation properties of unbound aggregates. In Proceedings, 7th International Conference on
396 the Bearing Capacity of Roads, Railways and Airfields, Trondheim, Norway.
- 397 36. Uthus L (2007) Deformation Properties of Unbound Granular Aggregate. PhD
398 dissertation, Norwegian University of Science and Technology.
- 399 37. Werkmeister S (2003) Permanent deformation behaviour of unbound granular materials in
400 pavement constructions. Thesis dissertation, Fakultät Bauingenieurweser der Technischen
401 Universität Dresden.
- 402 38. Werkmeister S, Dawson A, Wellner F (2004) Pavement design model for unbound
403 granular materials. *Journal of Transportation Engineering* 130(5):665-674.

404 39. Yang L, Powrie W, Priest J (2009) Dynamic stress analysis of a ballasted railway track
405 bed during train passage. *Journal of Geotechnical and Geoenvironmental Engineering*
406 135(5):680–689.

407

408

409 **List of Tables**

410 Table 1: Test program

411

412 **List of Figures**

413 Fig. 1: Grain size distribution of the studied materials

414 Fig. 2: Deviator stress versus axial strain for test ITL_5w6 - Determination of resilient modulus

415 Fig. 3: Deviator stress versus axial strain for test ITL_5w6 . a) $N = 1-8$ ($\Delta q_{max} = 45$ kPa); b) from

416 $\Delta q_{max} = 45$ kPa ($N = 30\ 000$) to $\Delta q_{max} = 90$ kPa ($N = 30\ 001 - 30\ 0004$); c) from $\Delta q_{max} = 90$ kPa

417 ($N = 60\ 000$) to $\Delta q_{max} = 145$ kPa ($N = 60\ 001 - 60\ 0004$); d) from $\Delta q_{max} = 145$ kPa ($N = 90\ 000$)

418 to $\Delta q_{max} = 20$ kPa ($N = 90\ 001 - 90\ 0004$)

419 Fig. 4: Resilient strain versus number of cycles in test $ITL_{10}w12$

420 Fig. 5: Resilient modulus versus number of cycles for ITL_{10} . a) $w = 4\%$; b) $w = 6\%$; c) $w = 12\%$

421 Fig. 6: Resilient modulus versus number of cycles for ITL_5w6

422 Fig. 7: Resilient modulus versus number of cycles for ITL_0 . a) $w = 4\%$; b) $w = 6\%$; c) $w = 12\%$

423 Fig. 8: Resilient modulus versus number of cycles for ITL_{-10} . a) $w = 4\%$; b) $w = 6\%$; c) $w = 12\%$

424 Fig. 9: End-stage resilient modulus versus deviator stress - Effect of water content. a) ITL_{10} ; b)

425 ITL_0 ; c) ITL_{-10}

426 Fig. 10: End-stage resilient modulus versus deviator stress - Effect of fines content. a) $w = 4\%$; b)

427 $w = 6\%$ and c) $w = 12\%$

428 Figure 11: Resilient modulus in function of water content at different fine contents; a) at $\Delta q_{max} =$

429 45 kPa and b) at $\Delta q_{max} = 140$ kPa

430

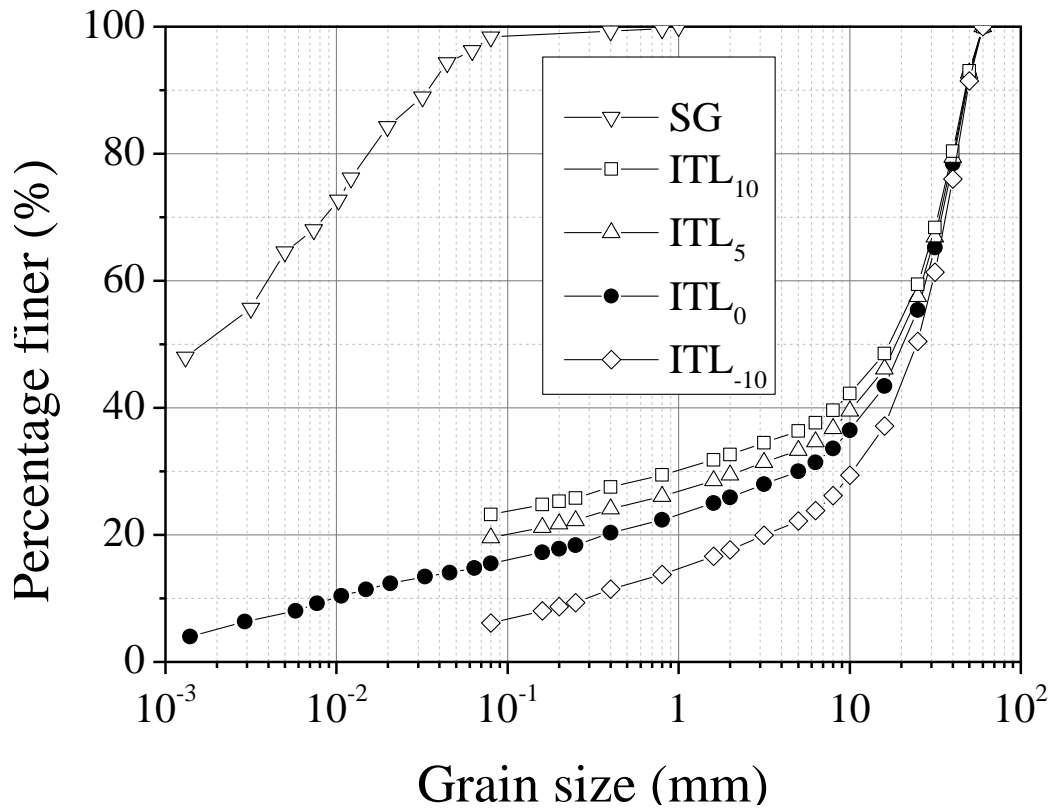
431

432

433 **Table 1: Test program**

Soil	Water content - w (%)		
	4 %	6 %	12 %
ITL ₁₀	ITL ₁₀ w4	ITL ₁₀ w6	ITL ₁₀ w12
ITL ₅	-	ITL ₅ w6	-
ITL ₀	ITL ₀ w4	ITL ₀ w6	ITL ₀ w12
ITL ₋₁₀	ITL ₋₁₀ w4	ITL ₋₁₀ w6	ITL ₋₁₀ w12

434
435
436
437

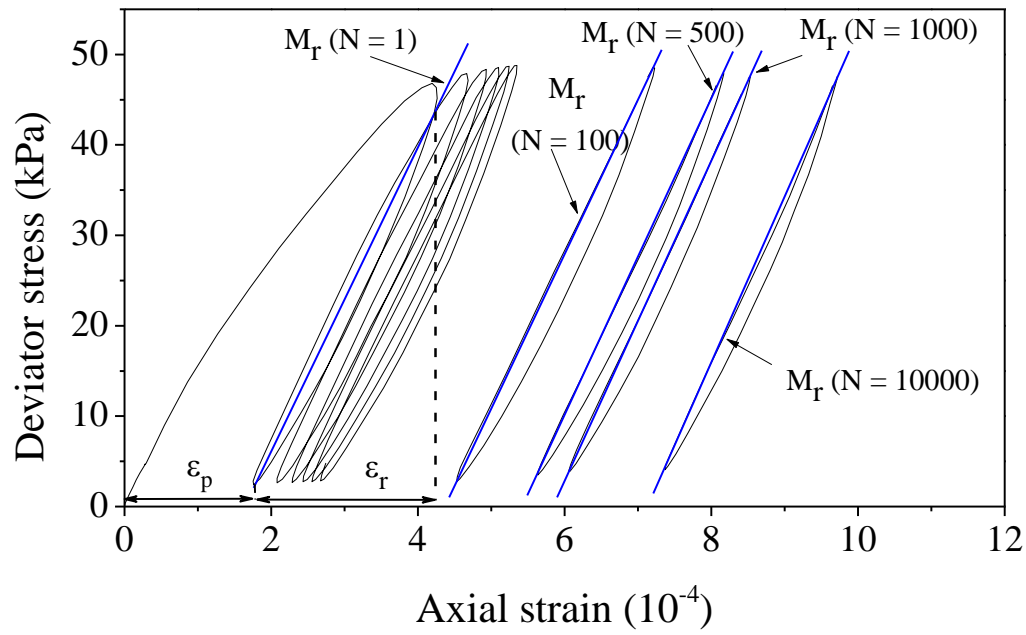


438

439 **Fig. 1: Grain size distribution of the studied materials**

440

441

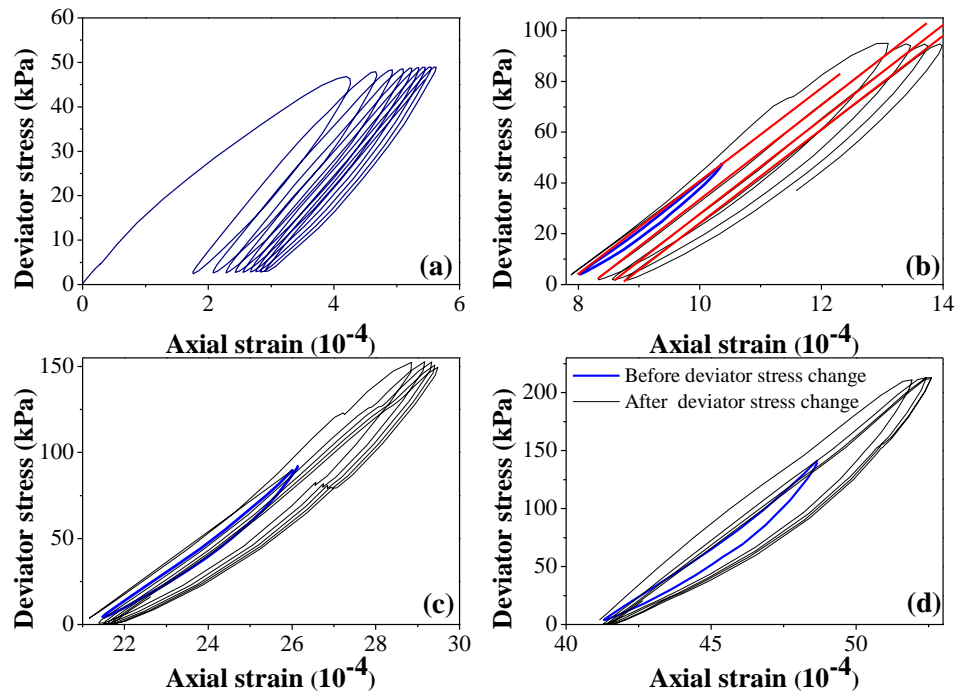


442

443 **Fig. 2: Deviator stress versus axial strain for test ITL₅w6 - Determination of resilient**
444 **modulus**

445

446

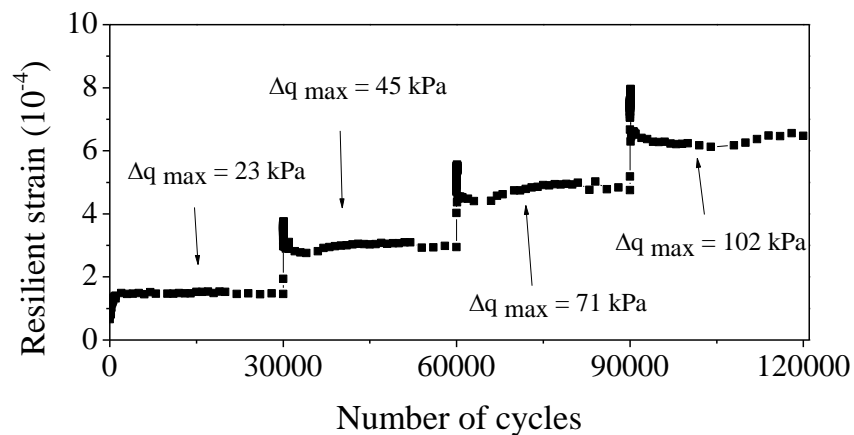


447

448 **Fig. 3: Deviator stress versus axial strain for test ITL₅w6. a) N = 1-8 ($\Delta q_{max} = 45$ kPa); b)**
 449 **from $\Delta q_{max} = 45$ kPa (N = 30 000) to $\Delta q_{max} = 90$ kPa (N = 30 001 - 30 0004); c) from $\Delta q_{max} =$**
 450 **90 kPa (N = 60 000) to $\Delta q_{max} = 145$ kPa (N = 60 001 - 60 0004); d) from $\Delta q_{max} = 145$ kPa (N**
 451 **= 90 000) to $\Delta q_{max} = 20$ kPa (N = 90 001 - 90 0004)**

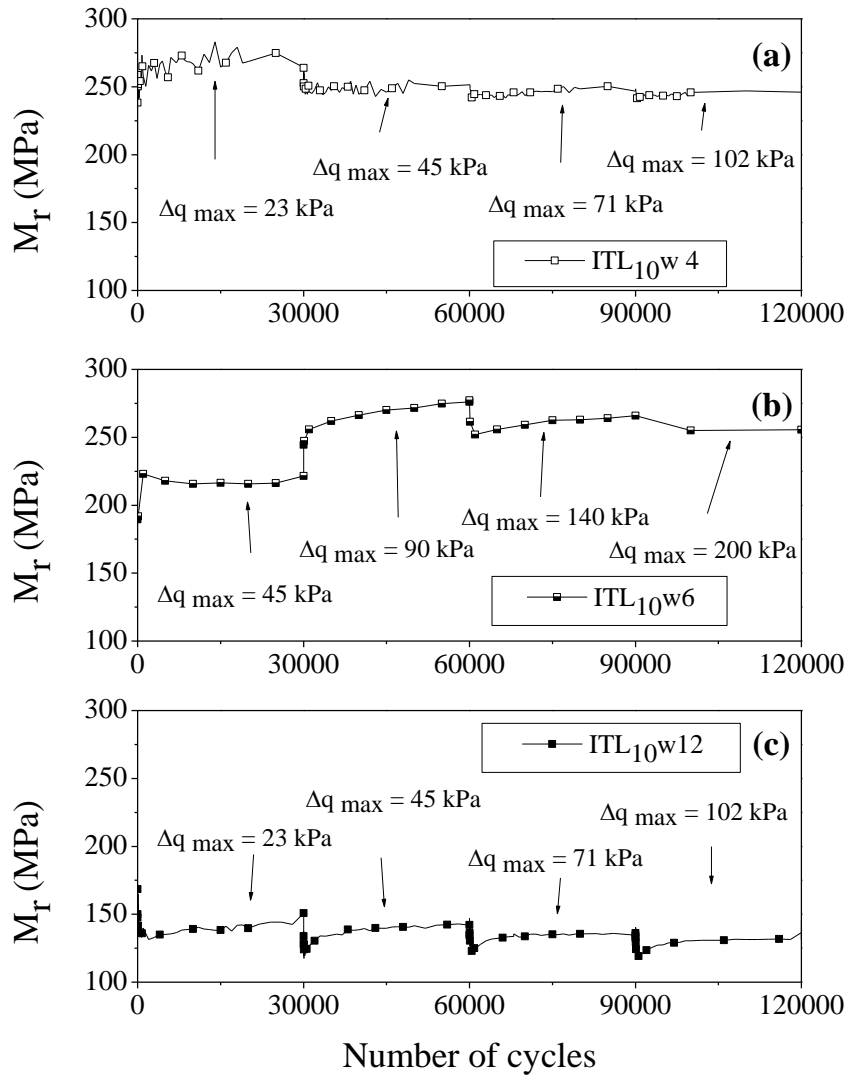
452

453



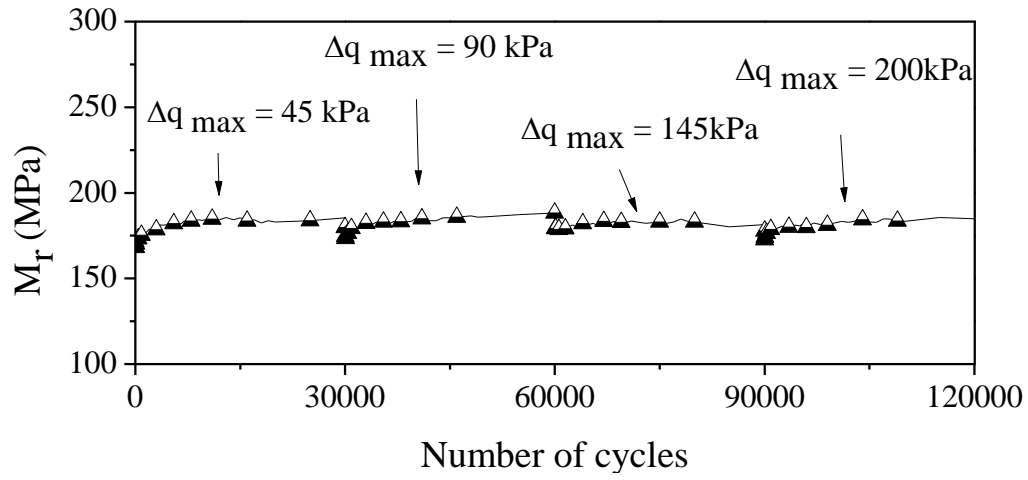
454

455 **Fig. 4: Resilient strain versus number of cycles in test ITL₁₀w12**



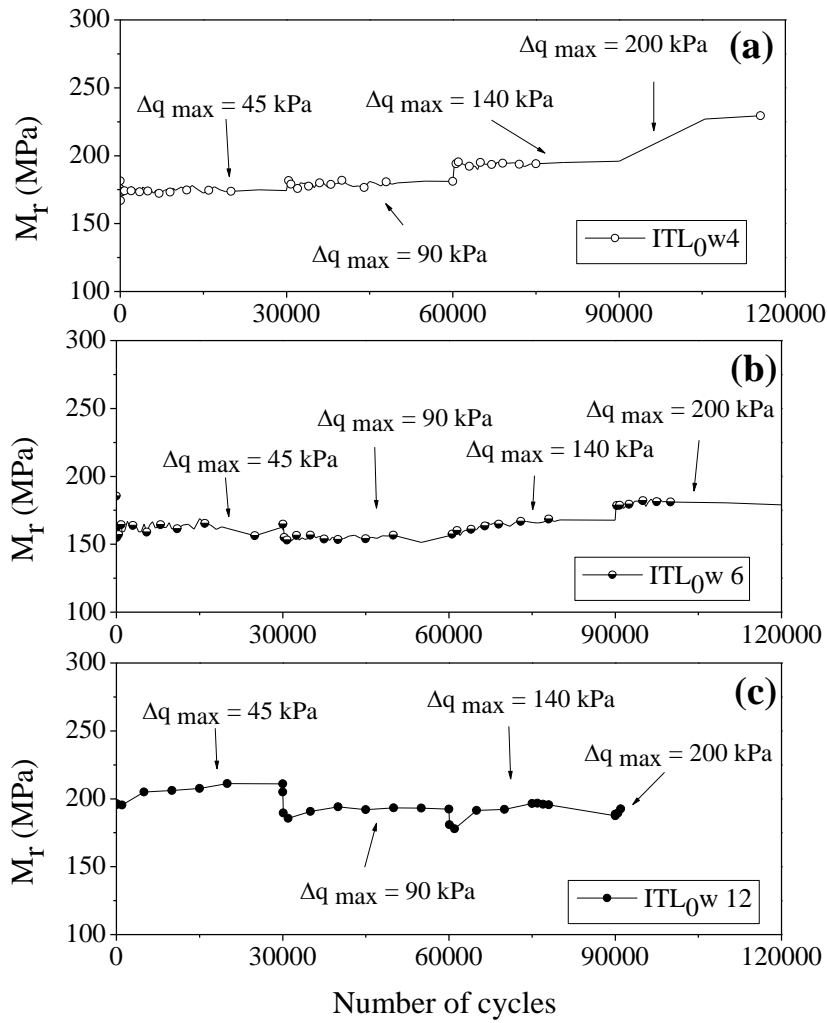
458 **Fig. 5: Resilient modulus versus number of cycles for ITL₁₀. a) $w = 4\%$; b) $w = 6\%$; c) $w =$**
 459 **12%**
 460

461



462

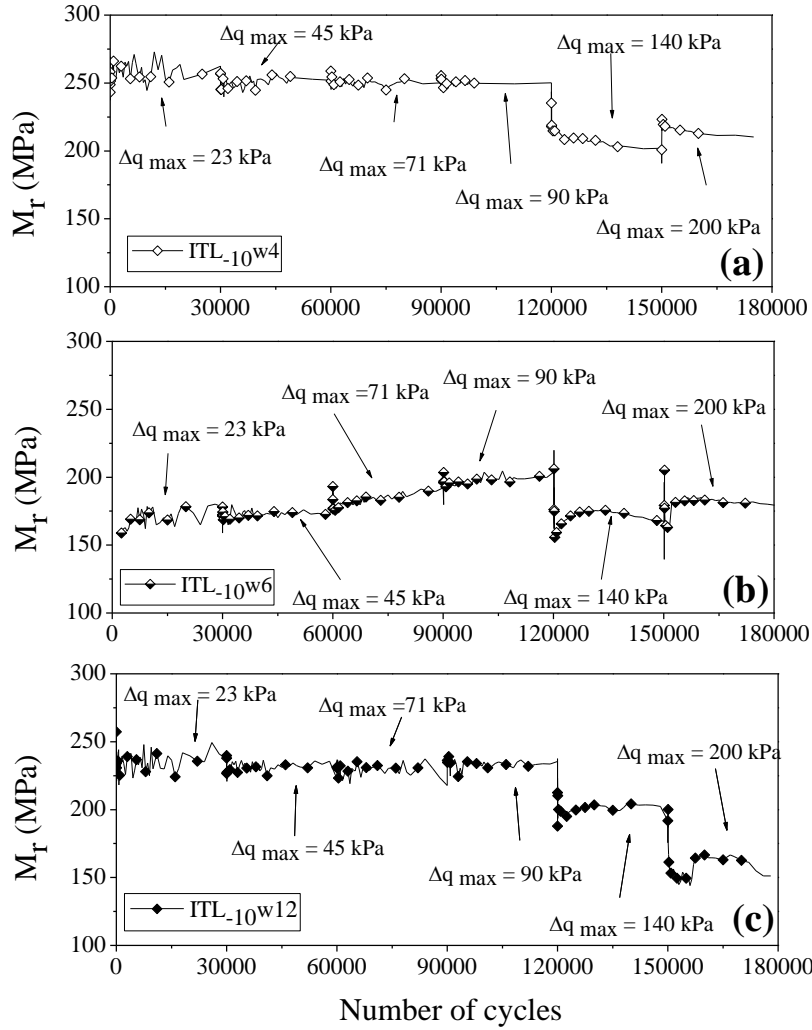
463 **Fig. 6: Resilient modulus versus number of cycles for ITL₅w6**



464

465 **Fig. 7: Resilient modulus versus number of cycles for ITL₀. a) $w = 4\%$; b) $w = 6\%$; c) $w =$**
 466 **12%**

467

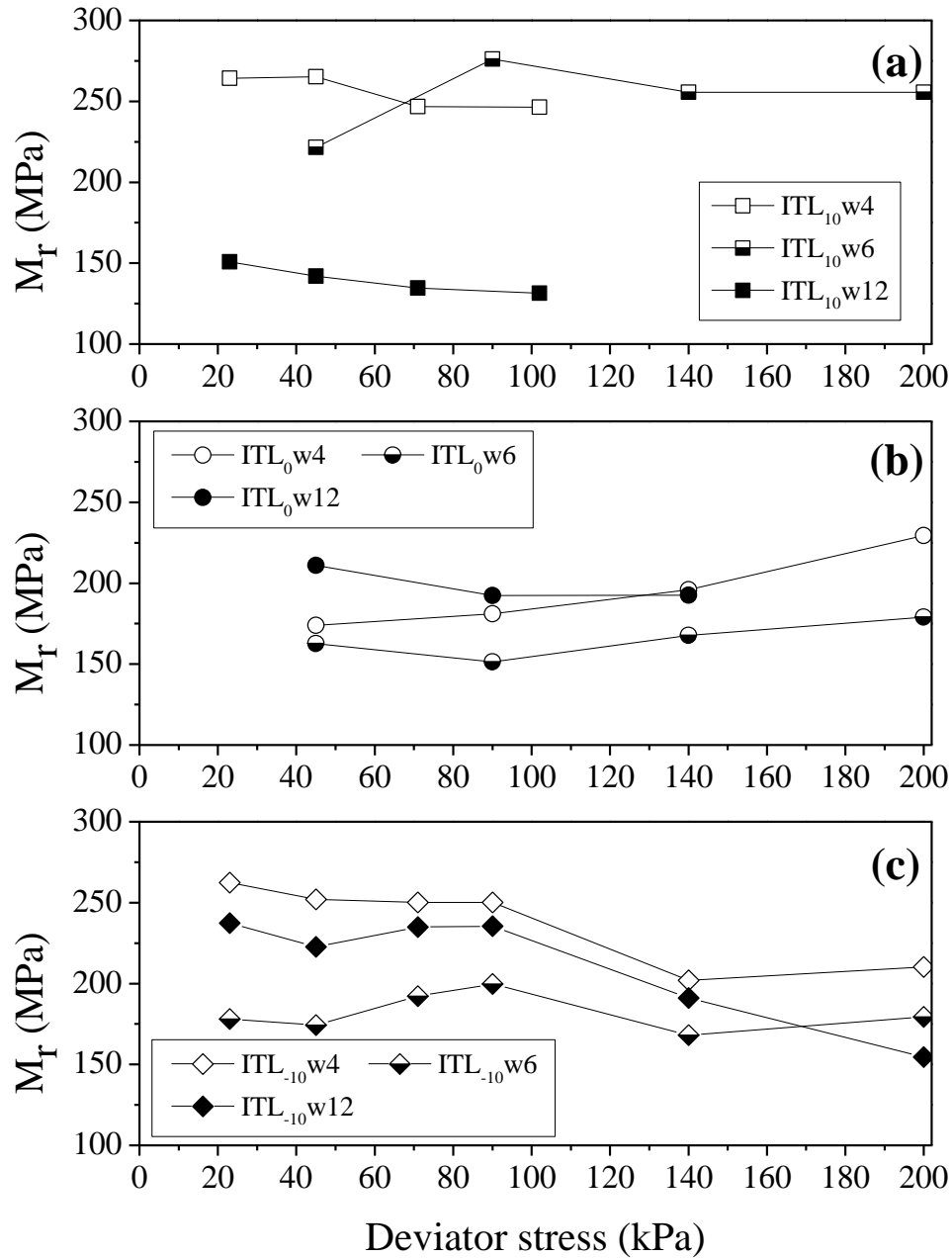


468

469 **Fig. 8: Resilient modulus versus number of cycles for ITL-10. a) $w = 4\%$; b) $w = 6\%$; c) $w =$**
 470 **12%**

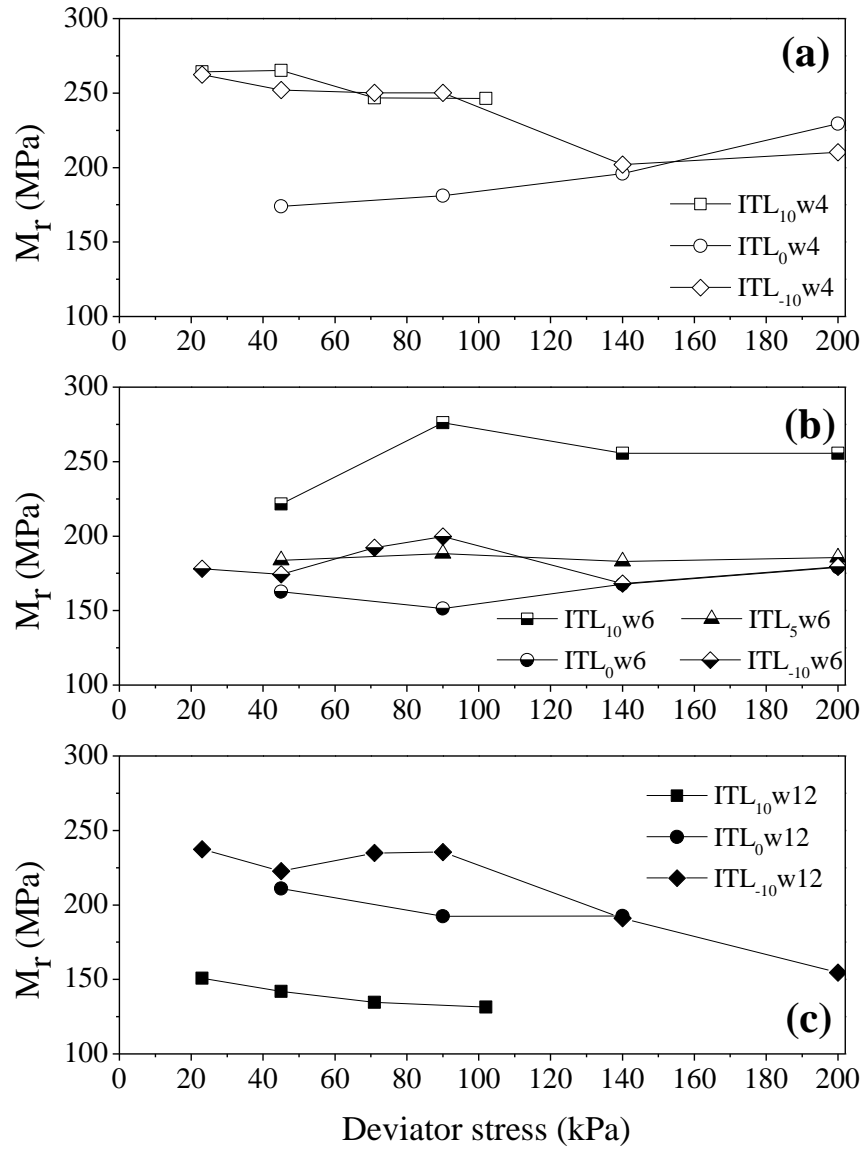
471

472



473

474 **Fig. 9: End-stage resilient modulus versus deviator stress - Effect of water content. a) $IITL_{10}$;**
 475 **b) $IITL_0$; c) $IITL_{-10}$**

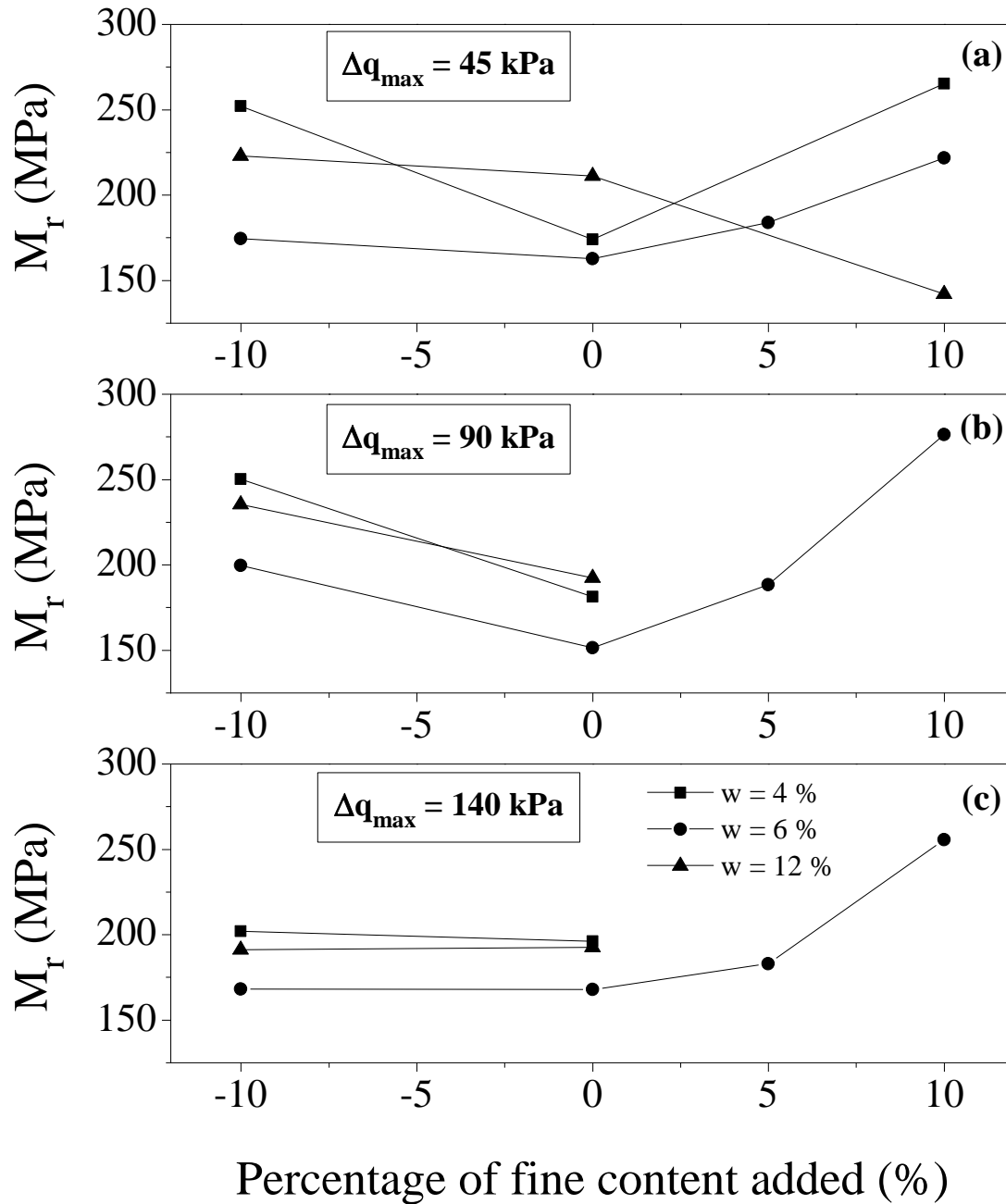


476

477 **Fig. 10: End-stage resilient modulus versus deviator stress - Effect of fines content. a) $w =$**
 478 **4%; b) $w = 6\%$ and c) $w = 12\%$**

479

480



481
 482 **Figure 11: Resilient modulus in function of water content at different fine contents; a) at $\Delta q_{max} = 45$ kPa; b) at**
 483 **$\Delta q_{max} = 90$ kPa and c) at $\Delta q_{max} = 140$ kPa**